

Incorporation of a Swirl into the k - ε Turbulence Model for Mathematical Simulations of Hydrodynamic Generators of Oscillations

A.S. Korneev

The A. A. Blagonravov Institute of Machine Science of the Russian Academy of Sciences, Moscow, Russia

ABSTRACT: *A mathematical model for the calculation of unsteady turbulent swirling flow in the presence of cavitation is presented. A correction for flow swirling in the k - ε turbulence model is proposed. Accounting for this amendment made it possible to achieve agreement between the calculated and experimental data on the pressure distribution along the channel wall of the hydrodynamic generator of oscillations and calculate amplitude-frequency characteristics.*

KEYWORDS: *Hydrodynamic generators of oscillations, Experiment, Calculation, Swirl effect in the k - ε -model of turbulence, Amplitude-frequency characteristics.*

Date of Submission: 05-06-2019

Date of acceptance: 20-06-2019

I. INTRODUCTION

Hydrodynamic generators of oscillations [1–3] produce waves when a fluid flows through channels of certain shape and dimensions. These generators have no any movable elements, which provides their reliability and service life. Mathematical modeling of such devices requires the calculation of unsteady turbulent swirling flows [4]. The standard k - ε turbulence model [5] does not take into account the effect of flow swirl on the flow characteristics. At the same time, there are experimental data that show that swirling leads to laminarization of the flow.

Murakami and Kikuyama [6] investigated the turbulent flow of water in a rotating tube. Water was fed into a long fixed pipe with a diameter of $D = 32$ mm and a length of $60D$, forming a steady-state turbulent longitudinal velocity profile. Untwisted flow got into the rotating tube and was involved in the rotation due to friction against the walls. The rotating tube had segments of different lengths: $30D$, $50D$, $70D$, $120D$, $140D$ and $160D$. Between these segments was located nozzles of total pressure, which could move along the radius. The velocity profile was determined from the magnitude of the dynamic pressure. Then the liquid fell into a fixed outlet tube with a length of $200D$. Measurements showed that, when moving along a rotating tube, the profile of the axial velocity component changed and was transformed from a steady-state turbulent to a parabolic, which is typical to a laminar flow.

Borisenko A. I., Kostikov O. N. and Chumachenko V. I. [7] using an anemometer with a hot wire were measured intensity of turbulent pulsations in a rotating pipe with a diameter of $D = 52$ mm, through which the air flow passed. It was found that a decrease in the intensity of the pulsations occurred in the rotating channel. This process began near the wall, and as the distance from the entrance extended to the central region of the pipe. Thus, under conditions typical of [6] and [7], swirl led to laminarization of the flow. This must be taken into account in the mathematical model.

In [8], experimental pressure distributions along the channel wall of a hydrodynamic oscillator were presented, which were compared with the calculated data using the model [4] and an amendment to the standard model of turbulence [5] was proposed, taking into account the swirl of the flow. In the present paper, based on this model, the calculated amplitude-frequency characteristics of hydrodynamic generators are obtained and compared with experimental characteristics.

II. OBJECT OF STUDY

The hydrodynamic generator (Fig. 1) had a cylindrical channel with an extension [8]¹. The working fluid (tap water) was fed through two tangential holes, providing a flow swirl. To measure the time-averaged pressure on the channel wall, 6 holes were made in the xz and yz planes. With the help of tubes, the holes were connected to pressure gauges.

¹ O. V. Shmyrkov performed the experiments in [8].

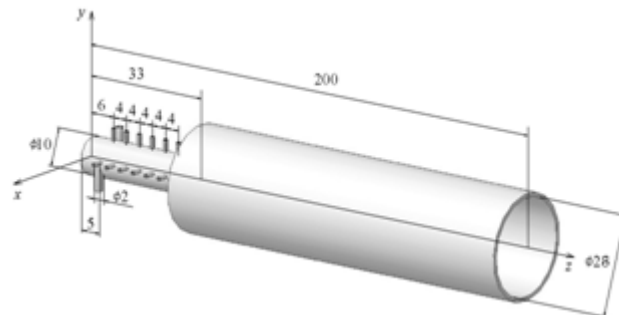


Figure 1. 3d-model of a hydrodynamic generator

III. MATHEMATICAL MODEL

The used system of governing equations was presented in [4]. This system has the averaged continuity and Navier–Stokes equations for an axisymmetric flow [9] and the $k-\varepsilon$ -model of turbulence [5].

$$\frac{\partial \rho}{\partial t} + \frac{\partial(\rho u)}{\partial z} + \frac{1}{r} \frac{\partial(r \rho v)}{\partial r} = 0; \tag{1}$$

$$\rho \frac{\partial u}{\partial t} + \rho u \frac{\partial u}{\partial z} + \rho v \frac{\partial u}{\partial r} = -\frac{\partial p}{\partial z} + \frac{\partial}{\partial z} \left(\mu_s \frac{\partial u}{\partial z} \right) + \frac{1}{r} \frac{\partial}{\partial r} \left(r \mu_s \frac{\partial u}{\partial r} \right); \tag{2}$$

$$\rho \frac{\partial v}{\partial t} + \rho u \frac{\partial v}{\partial z} + \rho v \frac{\partial v}{\partial r} = -\frac{\partial p}{\partial r} + \frac{\partial}{\partial z} \left(\mu_s \frac{\partial v}{\partial z} \right) + \frac{1}{r} \frac{\partial}{\partial r} \left(r \mu_s \frac{\partial v}{\partial r} \right) - \mu_s \frac{v}{r^2} + \rho \frac{w^2}{r}; \tag{3}$$

$$\rho \frac{\partial w}{\partial t} + \rho u \frac{\partial w}{\partial z} + \rho v \frac{\partial w}{\partial r} = \frac{\partial}{\partial z} \left(\mu_s \frac{\partial w}{\partial z} \right) + \frac{1}{r} \frac{\partial}{\partial r} \left(r \mu_s \frac{\partial w}{\partial r} \right) - \mu_s \frac{w}{r^2} - \rho \frac{v w}{r}. \tag{4}$$

$$\rho \frac{\partial k}{\partial t} + \rho u \frac{\partial k}{\partial z} + \rho v \frac{\partial k}{\partial r} = \frac{\partial}{\partial z} \left[\left(\mu + \frac{\mu_t}{\sigma_k} \right) \frac{\partial k}{\partial z} \right] + \frac{1}{r} \frac{\partial}{\partial r} \left[r \left(\mu + \frac{\mu_t}{\sigma_k} \right) \frac{\partial k}{\partial r} \right] + G - \rho \varepsilon; \tag{5}$$

$$\tag{6}$$

Here, $G = G_{u,v} + G_w$; $\mu_s = \mu + \mu_t$;

$$G_{u,v} = \mu_t \left\{ 2 \left[\left(\frac{\partial u}{\partial z} \right)^2 + \left(\frac{\partial v}{\partial r} \right)^2 + \left(\frac{v}{r} \right)^2 \right] + \left(\frac{\partial u}{\partial r} + \frac{\partial v}{\partial z} \right)^2 \right\}; G_w = \mu_t \left[\left(\frac{\partial w}{\partial z} \right)^2 + \left(r \frac{\partial}{\partial r} \left(\frac{w}{r} \right) \right)^2 - \frac{\partial}{\partial r} \left(\frac{w^2}{r} \right) \right];$$

$$C_1 = 1.44; C_2 = 1.92; C_\mu = 0.09;$$

$$\sigma_k = 1.0; \sigma_\varepsilon = 1.3.$$

In this work the turbulent viscosity μ_t was calculated taking into account the correction for the effect of swirl in the form [8]:

$$\mu_t = C_\mu \rho f_\mu \frac{k^2}{\varepsilon}; \tag{7}$$

$$f_\mu = 1 - \frac{w^2}{u^2 + v^2 + w^2}. \tag{8}$$

Here, u, v and w are axial, radial and tangential components of velocity, ρ is the liquid density, k is the turbulence kinetic energy, ε is the rate of dissipation of turbulence energy. In the absence of swirling ($w = 0$), the presented model of turbulence transfers into the standard one.

Cavitation was taken into account using the equation of transfer of the mass fraction of the vapor [10]

$$\rho \frac{\partial f_v}{\partial t} + \rho u \frac{\partial f_v}{\partial z} + \rho v \frac{\partial f_v}{\partial r} = R_{ce}. \tag{9}$$

Here, $f_v = \rho_v / (\rho_l + \rho_v)$ is the mass fraction of the vapor, ρ_l is the liquid density, $\rho_v = p_{sat} M_v / (RT)$ is the saturated vapor density, p_{sat} is the pressure of the saturated vapors of the liquid at a temperature T , M_v is the molar mass of the vapor, $p_v = p_{sat} + p_{turb} * 0.5$ is the effective pressure of the saturated vapor, $p_{turb} = 0.39 \rho k$ is the turbulent pressure, R_{ce} is the rate of liquid evaporation ($R_{ce} > 0$) or vapor condensation ($R_{ce} < 0$), and

$$\begin{aligned}
 p \leq p_v: \quad R_{ce} &= C_e \frac{\rho_l \rho_v}{\sigma} (1 - f_v) \sqrt{\frac{2(p_v - p)k}{3\rho_l}}; \\
 p > p_v: \quad R_{ce} &= -C_l \frac{\rho_l \rho_v}{\sigma} (1 - f_v) \sqrt{\frac{2(p - p_v)k}{3\rho_l}}; \\
 \rho &= \left(\frac{f_v}{\rho_v} + \frac{1 - f_v}{\rho_l} \right)^{-1}; \quad \mu = \left(\frac{f_v}{\mu_v} + \frac{1 - f_v}{\mu_l} \right)^{-1};
 \end{aligned}$$

Here, ρ is the effective density of the working medium (mixture of liquid and vapor), μ is the effective dynamic viscosity of the working medium, σ is the coefficient of the surface tension of the liquid, $C_e = 0.02$, $C_l = 0.01$ are the empirical constants. The rest of the notation is generally accepted.

The system of equations (1) - (9) was solved using the method of pressure corrections [11], together with the SIMPLE algorithm. In this method the equation for pressure corrections p' derived on the basis of the continuity equation is solved rather than the continuity equation itself. As a steady-state solution is attained in the iteration procedure in the pressure, the corrections p' tend to zero. The calculations were carried out for the cylindrical channel of a generator, $R_c = 5$ mm in radius and $L_c = 33$ mm in length; at the channel exit there was a chamber, or an expansion section, $R_k = 14$ mm in radius and $L_k = 167$ mm in length (Fig. 2).

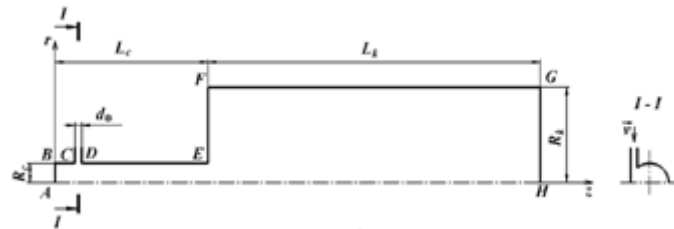


Figure 2. Diagram of the computational domain; AB and EF are end walls, BC, DE, and FG are cylindrical walls, GH is the exit section, CD is the liquid supply region, and AH is the axis of symmetry.

The no-slip conditions were imposed on the solid walls AB, BC, DE, EF, and FG (Fig. 2): $u = v = w = 0$, $p' = 0$, $\partial p / \partial n = 0$, $k = 0$, $\partial \varepsilon / \partial n = 0$ and $f_v = 0$; here, n is the coordinate along the normal to the wall. In the wall zones the turbulent kinetic energy dissipation rate ε_p was calculated on the basis of the wall functions [12]

$$\begin{aligned}
 y^* < y_v^*: \quad \varepsilon_p &= \frac{2\mu_p k_p}{\rho_p \sqrt{y_v}}, \\
 y^* \geq y_v^*: \quad \varepsilon_p &= \frac{k_p \sqrt{k_p}}{C_1 y_p}, \\
 y^* &= \frac{y_p \rho_p \sqrt{k_p}}{\mu_p}, \quad y_v = y_v^* \frac{\mu_p}{\rho_p \sqrt{k_p}}.
 \end{aligned}$$

rather than by means of solving the differential equation (6). Here, y_p is the dimensional distance from the wall, y_v and y_v^* are dimensionless coordinates, $y_v^* = 20$, k_p is a turbulent kinetic energy in the wall zone, and ρ_p and μ_p are the density and the laminar viscosity in the wall zone.

The following conditions are preassigned at the axis of symmetry

$$\partial u / \partial r = 0, \quad v = 0, \quad w = 0, \quad \partial p' / \partial r = 0, \quad \partial p / \partial r = 0, \quad \partial k / \partial r = 0, \quad \partial \varepsilon / \partial r = 0, \quad \partial f_v / \partial r = 0.$$

In the liquid entry region CD we have

$$\begin{aligned}
 u &= 0, \quad v = Q / (2\pi R_c d_0), \quad w = 4 \cdot Q / (\pi d_0^2 \cdot n_0), \quad p' = 0, \quad \partial p / \partial r = 0, \quad k = k_0, \quad \varepsilon = \varepsilon_0, \quad k_0 = (k_{in} v_0)^2 / 2, \\
 \varepsilon_0 &= C_\mu k_0 \sqrt{k_0} / (0.1 d_0); \text{ here, } n_0 \text{ is the number of the supply orifices, } n_0 = 2, \quad k_{in} = 0.05.
 \end{aligned}$$

At the exit GH we have $p = p_{out}$ and the “soft” boundary conditions $\partial F / \partial z = 0$, where F is any of the variables $u, v, w, p', k, \varepsilon$, and f_v .

IV. RESULTS AND DISCUSSION

The calculations were carried out with the absolute water pressure at the inlet of the generator $p_{in} = 5.1$ MPa, the outlet pressure $p_{out} = 0.24$ MPa. The fluid flow was equal to $Q = 23.3 \text{ dm}^3 / \text{min}$, the Reynolds number calculated from the average velocity in the channel, $Re \approx 5000$. These parameters corresponded to the experimental conditions [8, 13]. The experimental setup was presented in [13]. The thermophysical properties of the working fluid (water) were taken according to the data of [14].

4.1. Time dependences of the pressure.

The calculated time dependences of the pressure p at the axis $r = 0$ are presented in Fig. 3 for the following characteristic sections: $z = 5 \text{ mm}$, the section of supply orifices (middle of the CD region in Fig. 2), in the output section at the nozzle exit of the generator ($z = 33 \text{ mm}$) and the point in which the pressure transducer was located in the experiment [13] ($z = 100 \text{ mm}$, $r = 14 \text{ mm}$)

Calculations without a correction for the swirl, $f_{\mu} = 1$ (Fig. 3) lead to a damping of pressure oscillations over time, whereas in the experiments [13] these oscillations existed constantly. Calculations taking into account the swirl correction (Fig. 4) give steady-state fluctuations in time. In the calculation without a correction for the swirl after reaching the stationary mode, the pressure did not fall below the saturated vapor pressure $p_{sat} = 2.3 \text{ kPa}$ (at $t = 20 \text{ }^{\circ}\text{C}$ [14]) at any of the points considered. This means, that at the considered values of parameters in the channel of the generator there was no cavitation. At the same time, experiments [13] showed the presence of traces of erosion of the material, which indicated the presence of cavitation. The calculation taking into account the correction for the swirl by the formula (8) revealed the presence of undamped pressure fluctuations (Fig. 4). In addition, the calculated pressure in some areas turned out to be lower than the saturated vapor pressure; therefore, cavitation occurred in these areas, which agrees with the experimental data [13].

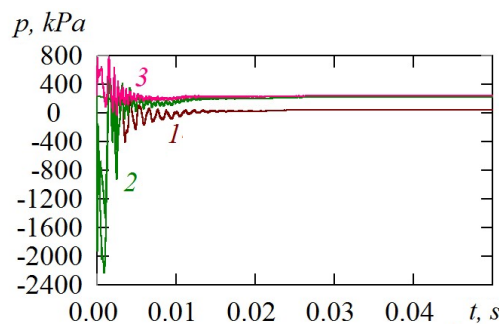


Figure 3. Calculated dependences of pressure on time without correction for swirl ($f_{\mu} = 1$),

Coordinate values are 1 - $z = 5 \text{ mm}$, $r = 0 \text{ mm}$, 2 - $z = 33 \text{ mm}$, $r = 0 \text{ mm}$, 3 - $z = 100 \text{ mm}$, $r = 14 \text{ mm}$.

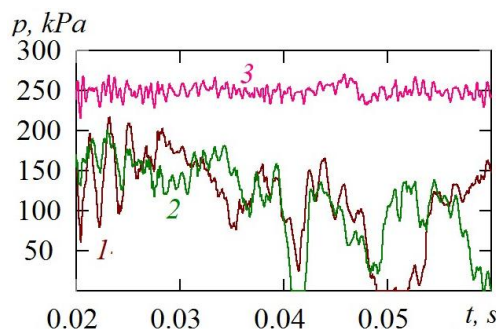


Figure 4. Calculated dependences of pressure on time with correction for the swirl (f_{μ} is according to the formula (8)).

Coordinate values are 1 - $z = 5 \text{ mm}$, $r = 0 \text{ mm}$, 2 - $z = 33 \text{ mm}$, $r = 0 \text{ mm}$, 3 - $z = 100 \text{ mm}$, $r = 14 \text{ mm}$.

4.2. Amplitude-frequency characteristics.

By decomposing in a Fourier series the data shown in Fig. 4, line 3, the calculated amplitude-frequency characteristics (AFC) of the generator were obtained (Fig. 5, line 1). The corresponding experimental frequency response according to [13] is shown in Fig. 5, line 2. At the experimental frequency response two main maxima are clearly distinguished at frequencies $f = 1040 \text{ Hz}$ and $f = 1980 \text{ Hz}$. On the calculated frequency response they correspond to maxima at $f = 978 \text{ Hz}$ (6% difference) and two closely spaced maxima at $f = 1689$ and 1956 Hz

(15% difference and 2%, respectively). Experimental frequency response (Fig. 5, line 2) was measured in [13] using a Kistler Company pressure sensor and a Lecroy WaveSurfer oscillograph.

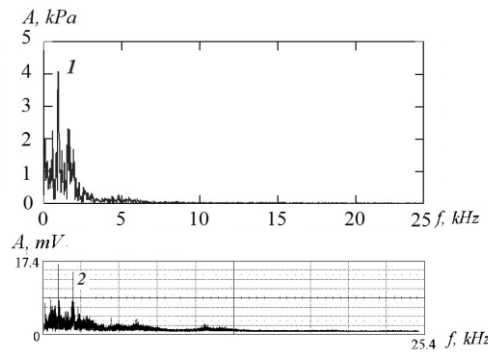


Figure 5. Calculated (1) and experimental (2) amplitude-frequency characteristics.

4.3. Pressure distribution along the channel wall.

The experimental pressure distributions [8] along the wall of the generator channel in the xz plane are shown in Fig. 6, points 1, and in the yz plane in Fig. 6, points 2. It can be seen that deviations from axisymmetry appear up to distances $z = 10 - 12$ mm from the left end wall of the channel. The calculations without taking into account the correction for the flow swirl (Fig. 6, line 3) showed a noticeable deviation from the experimental values. The calculated data obtained in the axisymmetric approximation with the swirl correction (Fig. 6, line 4) are between the experimental points for the xz and yz planes.

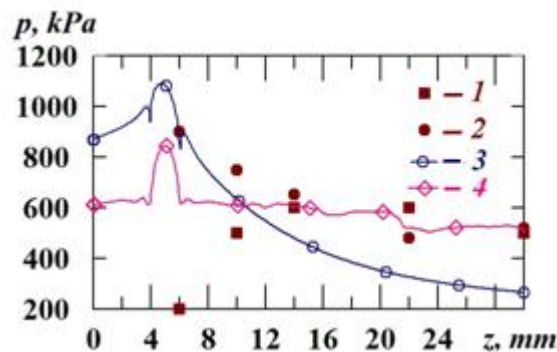


Figure 6. The distribution of the time averaged pressure on the wall of the generator channel: experiments in the xz (1) and yz (2) plane, calculations without the swirl correction (3) and with the swirl correction (4).

V. CONCLUSION

A correction for flow swirl in the $k-\varepsilon$ turbulence model is proposed. Accounting for this amendment made it possible to achieve agreement between the calculated and experimental data on the pressure distribution along the channel wall of the hydrodynamic generator, revealed the presence of cavitation in the generator under study, and made it possible to calculate the amplitude-frequency characteristics of the oscillations. In the absence of swirl, the presented model automatically changes to the standard one.

Calculations for the $k-\varepsilon$ turbulence model without taking into account the swirl correction led to the damping of pressure oscillations with time, while in the experiments these oscillations were observed. Calculations taking into account the swirl correction gave steady-state oscillations in time and allowed us to calculate the amplitude-frequency characteristics of these oscillations, the positions of the main maxima of which are in agreement with the experimental data.

The obtained data can be used in calculations of turbulent swirling flows, in particular, in the design of hydrodynamic generators of oscillations.

VI. ACKNOWLEDGEMENT

The author is grateful to the head of the Nonlinear Wave Mechanics and Technology Center of the RAS - the Branch of the A. A. Blagonravov Institute of Machine Science, Russian Academy of Sciences, academician R. F. Ganiev, as well as the Center team for the help and useful work discussions. The author is especially grateful to O. V. Shmyrkov for the provided experimental data.

REFERENCES

- [1]. V. S. Avduevskii, R. F. Ganiev, G. A. Kalashnikov, S. A. Kostrov, R. S. Mufazalov, Hydrodynamic Generator of Oscillations: RF Patent 2015749, Byull. Izobret., no. 13, p.34, 1994. (in russian)
- [2]. R. F. Ganiev, D. A. Zhebynev, A. S. Korneev, and L. E. Ukrainskii, Wave Dispersion of a Gas in a Liquid, Fluid Dynamics, 43(2), 2008, 297-302.
- [3]. R. F. Ganiev, L. E. Ukrainski, Nonlinear wave mechanics and oscillatory phenomena on the basis of high technologies (Begell house, USA, 2012).
- [4]. A. S. Korneev, Mathematical Simulation of Hydrodynamic Generators of Oscillations, Fluid Dynamics, 48(4), 2013, 471-476.
- [5]. B. E. Launder, D. B. Spalding, The numerical computation of turbulent flows, Comput. Methods in Appl. Mech. and Eng., 3(2), 1974, 269-289.
- [6]. Mitsukiyo Murakami, Kouji Kikuyama, Turbulent Flow in Axially Rotating Pipes, Trans. ASME. J. Fluids Eng., 102(1), 1974, 97-103.
- [7]. A. I. Borisenko, O. N. Kostikov, V. I. Chumachenko, Experimental Study of turbulent flow in a rotating channel., Journal of Engineering Physics, 24(6), 1973, 770-773.
- [8]. A. S. Korneev, Mathematical Simulation of Hydrodynamic Generators of Oscillations, Proc. International Conf. "Machines, technologies and materials for modern machinery", dedicated to the 80th anniversary of the Blagonravov Institute of Machine Science of RAS, Moscow, Russia, 2018, 95 (in russian)
- [9]. H. Schlichting, Boundary-Layer Theory (McGraw-Hill, Inc., New York, USA, 1979)
- [10]. A. K. Singhal, M. M. Athavale, H. Y. Li, Y. Jiang, Mathematical basis and validation of the full cavitation model, J. Fluids Eng. – Trans. ASME, 124(3), 2002, 617-624.
- [11]. S. V. Patankar, Numerical Heat Transfer and Fluid Flow (McGraw-Hill, Hemisphere Publishing Corporation, 1980).
- [12]. T. J. Craft, A. V. Gerasimov, H. Iacovides, B. E. Launder, Progress in the generalization of wall-function treatments, Int. J. Heat and Fluid Flow, 23(2), 2002, 148-160.
- [13]. R. F. Ganiev, O. V. Shmyrkov, N. V. Gun, Behavior Features of Cavitation Processes in a Through-Flow Wave Vortex Generator, Doklady Physics, 59(2), 2014, 86-88.
- [14]. N. B. Vargaftik, Handbook of Physical Properties of Liquids and Gases. Pure Substances and Mixtures (Springer, New York, USA, 1975)

A.S. Korneev" Incorporation of a Swirl into the k - ε Turbulence Model for Mathematical Simulations of Hydrodynamic Generators of Oscillations" International Journal of Research in Engineering and Science (IJRES), vol. 07, no. 1, 2019, pp. 29-34